

Exchange bias through a Cu interlayer in an IrMn/Co system

J. Geshev,¹ S. Nicolodi,¹ L. G. Pereira,¹ L. C. C. M. Nagamine,¹ J. E. Schmidt,¹ C. Deranlot,² F. Petroff,²
R. L. Rodríguez-Suárez,³ and A. Azevedo³

¹*Instituto de Física, Universidade Federal do Rio Grande do Sul, 91501-970 Porto Alegre, Rio Grande do Sul, Brazil*

²*Unité Mixte de Physique CNRS/Thales, 91767 Palaiseau, France and Université Paris-Sud, 91405 Orsay, France*

³*Departamento de Física, Universidade Federal de Pernambuco, 50670-901 Recife, Pernambuco, Brazil*

(Received 3 May 2007; revised manuscript received 14 May 2007; published 1 June 2007)

Ferromagnetic resonance (FMR) and magnetization (MAG) measurements were used to study the exchange interaction between the antiferromagnetic and ferromagnetic layers in an IrMn/Cu/Co system as a function of the Cu spacer thickness. Although the experimental angular variations of the exchange-bias fields H_{eb}^{FMR} and H_{eb}^{MAG} coincide, the coupling strengths J and the Co layers' anisotropy fields H_U , obtained via numerical simulations, are different. For all Cu thicknesses $J^{FMR} > J^{MAG}$ and $H_U^{FMR} < H_U^{MAG}$. The exchange coupling decreases exponentially with the spacer thickness and is a short-range interaction. These characteristics were explained in the framework of a model considering polycrystalline magnetic layers with independent easy axis distributions, taking into account the rotatable anisotropy. The role of antiferromagnetic grains at the interface with different sizes and different magnetic stabilities is essential for understanding the behavior of this exchange-biased system.

DOI: 10.1103/PhysRevB.75.214402

PACS number(s): 75.30.Gw, 71.70.Gm, 75.60.-d, 76.50.+g

I. INTRODUCTION

Although the exchange coupling between ferromagnetic (FM) and antiferromagnetic (AF) materials has been extensively studied in the past two decades due to its determinant role in the exchange-bias (EB) phenomenon,¹ many of its characteristics remain unclear. For example, there still exists a controversy with respect to whether the AF/FM interactions are long² or short range.³ Also, the fact that different measurement techniques may yield distinct values for the exchange anisotropy⁴⁻¹³ has been attributed to twisting of the magnetization through the thickness of the FM film,⁴ to different numbers of stable AF moments at the AF/FM interface in low and high field measurements,¹¹ or to the inconsistency of the model used to interpret the experiment.¹² It has been shown that the exchange-bias fields, derived from reversible and irreversible measurements, must, in general, be different.¹³

In this paper, we show that the EB fields obtained by ferromagnetic resonance (FMR) and magnetization (MAG) measurements on our IrMn/Cu/Co films are *equal* and the coupling strengths and the FM anisotropy, estimated via model calculations, are *different* unless the direct AF/FM contact coupling is very weak. We demonstrate that the magnetic stability of the interfacial AF grains is essential for understanding such a behavior.

II. EXPERIMENT

Ru/IrMn(15 nm)/Cu(t_{Cu})/Co(5 nm)/Ru films, where the thickness t_{Cu} of the Cu layer has been varied between 0 and 5 nm, were deposited by magnetron sputtering (base pressure of 5.0×10^{-8} mbar, Ar pressure of 2.5×10^{-3} mbar for the deposition of Ru, Cu, and Co, and 1.0×10^{-2} mbar for IrMn) onto Si(100) substrates. In order to enhance the exchange-bias effect, the samples were submitted to posterior magnetic annealing for 15 min at 200 °C in Ar atmo-

sphere with magnetic field of 1.6 kOe applied in the plane of the films.

Conventional x-ray diffractometry analysis identified (111) texture of the IrMn and Co layers, promoted by the Ru buffer. The Cu (111) peak moved to a smaller angle, as compared to its bulk value, suggesting a Cu lattice expansion, which follows the IrMn face-centered-cubic structure as well.

Alternating gradient field magnetometry (AGFM) has been used for the magnetic characterization of the samples.^{14,15} FMR data were obtained with an X-band spectrometer operating at the microwave excitation frequency ω of 8.61 GHz, with the sample mounted on the tip of an external goniometer to allow measurement of the in-plane resonance field H_{res} as a function of the in-plane field angle ϕ_H . The latter is equal to zero for dc magnetic field H applied along the EB direction. The samples' preparation and their characterization were performed at room temperature, and in all measurements, H was applied in the film's plane.

III. RESULTS AND DISCUSSION

Very recently,¹⁴ the thickness dependence of the EB field, H_{eb}^{MAG} (i.e., the magnetization curve's field shift), and coercivity H_c of these films were investigated through AGFM. Rapid decrease of both H_{eb}^{MAG} and H_c was observed when increasing the spacer thickness, and also that for $t_{Cu} \geq 1.5$ nm, the magnetic layers are practically decoupled. None of the samples showed training effects. The magnetization curves and FMR characteristics of the sample without Cu layer and the one with $t_{Cu}=0.25$ nm are very similar. Representative easy and hard magnetization curves as well as $H_{eb}^{MAG}(\phi_H)$ for $t_{Cu}=0.25$ nm are plotted in Fig. 1.

To obtain the anisotropy parameters and the AF/FM interaction strength in such complex systems, i.e., films composed of two *interacting* magnetic phases, it is indispensable to perform model simulations that fit the experimental data.

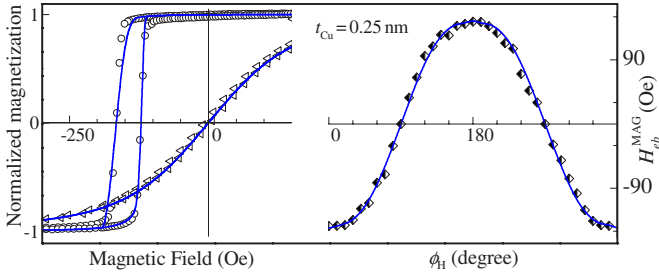


FIG. 1. (Color online) Left: In-plane magnetization curves for the sample with $t_{\text{Cu}}=0.25$ nm for field along the easy (circles) and hard (triangles) directions; right: the corresponding $H_{\text{res}}^{\text{MAG}}$ angular variation (diamonds). The lines are the best-fitting curves obtained using $H_U=65$ Oe, $H_W=510$ Oe, $H_E=142$ Oe, $H_{RA}=14$ Oe, $\sigma_{\text{AF}}=0.12$ rad, and $\sigma_{\text{FM}}=0.10$ rad.

In order to reproduce the rounded shape of the magnetization curves, one has to assume partly disordered interface moments by considering certain easy axis direction distributions (with standard deviation σ). Each exchange-coupled AF/FM pair was assumed to obey the model^{12,16} of Mauri *et al.*, which has the FM uniaxial anisotropy field $H_U(=2K/M)$, the AF domain-wall anisotropy field $H_W[=\sigma_W/(tM)]$, and the coupling field $H_E[=J/(tM)]$ as parameters. It is worth emphasizing that H_E , an intrinsic property of the AF/FM system, is different from H_{eb} which, in general, depends on J , H_U , and H_W .¹² Here, t is the thickness of the Co layer, and M and K are its saturation magnetization and uniaxial anisotropy constant, respectively, J is the AF/FM coupling constant, and σ_W is the energy per unit surface of an AF domain wall. The calculations for the as-made sample with $t_{\text{Cu}}=0$ nm have indicated that the AF part of the interface is almost fully spin compensated (though disordered) and nearly uncompensated after annealing, and that the annealing improved the interfacial IrMn spin alignment without changing the Co anisotropy.¹⁴

Our fittings of the FMR data (see below) showed that there is an additional field acting on the samples, i.e., the rotatable anisotropy field $H_{RA}(=2K_{RA}/M)$, a field that rotates to be parallel to the equilibrium direction of the FM magnetization and is responsible for the frequently observed resonance field shift.⁶ This originates from the unstable AF magnetic moments at the interface and can substantially change the shape of the magnetization curves and their characteristics.¹⁷ Here, we used H_{RA} as an additional parameter in both magnetization and FMR simulations. The magnetic free energy per unit area can be written as

$$E = -\mathbf{H} \cdot \mathbf{M} + 2\pi(\mathbf{M} \cdot \hat{\mathbf{n}})^2 - K \frac{(\mathbf{M} \cdot \hat{\mathbf{u}})^2}{M^2} - K_{RA} \frac{(\mathbf{M} \cdot \hat{\mathbf{h}})^2}{M^2} - \sigma_W \frac{\mathbf{M}_{\text{AF}} \cdot \hat{\mathbf{u}}_{\text{AF}}}{M_{\text{AF}}} - J \frac{\mathbf{M} \cdot \mathbf{M}_{\text{AF}}}{M M_{\text{AF}}}, \quad (1)$$

where the first four terms are the Zeeman, demagnetizing, FM uniaxial, and rotatable anisotropy energies, respectively. The last two terms are the AF domain-wall anisotropy and the AF/FM exchange coupling. The unit vectors $\hat{\mathbf{u}}$ and $\hat{\mathbf{u}}_{\text{AF}}$

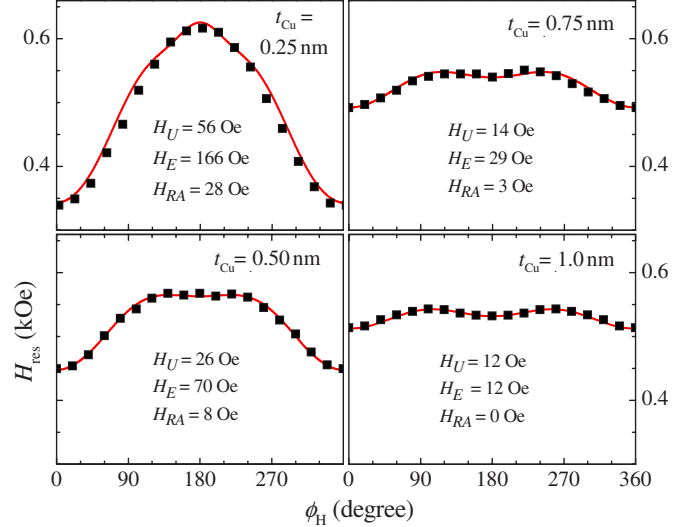


FIG. 2. (Color online) Angular variations of the resonance field for different t_{Cu} . Symbols represent the experimental data and the lines are calculated using the parameters given in each panel as well as $H_W=510$ Oe and $M_{\text{Co}}=1372$ emu/cm³.

represent the FM and AF layers' uniaxial anisotropy directions, respectively; $\hat{\mathbf{n}}$ and $\hat{\mathbf{h}}$ are the normal to the film surface and the applied field directions, respectively. The value of 1372 emu/cm³ for M of Co, estimated from the fitting of $H_{\text{res}}(\phi_H)$ for the film with $t_{\text{Cu}}=1.0$ nm (for which $H_{RA}=0$), was subsequently used in all simulations. In the latter, the normalized (to their saturation values) magnetizations, i.e., the cosines of the angles between \mathbf{M} (and \mathbf{M}_{AF}) and \mathbf{H} , are obtained by minimizing the energy given by Eq. (1); details on the numerical procedure employed can be found in Refs. 12 and 13.

The best-fitting magnetization curves for $t_{\text{Cu}}=0.25$ nm are plotted in Fig. 1. Note that independent AF and FM easy axis distributions were used. There is very good agreement between model and experiment for both easy and hard directions, and the same holds for $H_{\text{res}}^{\text{MAG}}(\phi_H)$, confirming that the magnetic behavior of such IrMn/Co systems can be very well explained using coherent rotation models.¹⁸ Since the AF layers were first deposited, their intrinsic anisotropy should not change distinctly after the subsequent growth of the Cu layers independently of their thickness, so $H_W=510$ Oe was used for all t_{Cu} . Although easy axis distributions have been used in the magnetization curve calculations only, the same energy expression has been employed in both MAG and FMR simulations.

The full squares in Fig. 2 represent the angular variations of the experimentally measured resonance fields. The lines in this figure give the corresponding best-fitting curves, calculated with the help of the previously derived¹³ [for the energy given by Eq. (1)] expression for $H_{\text{res}}(\phi_H)$ and using the parameters given in each panel. It is worth noting that the above cited analytical expression depends not only on M , t , H_U , H_W , J , and ω , but also on the equilibrium angles of \mathbf{M} and \mathbf{M}_{AF} . Here, these angles were estimated using the same numerical procedure as that employed in the magnetization curve fittings obtained in the present work.

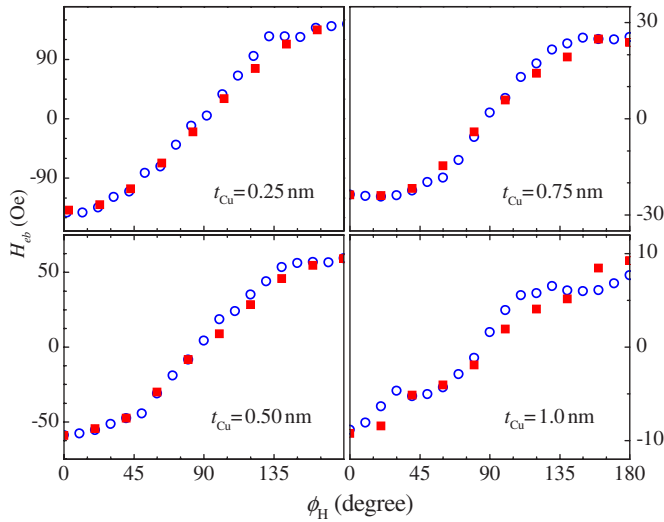


FIG. 3. (Color online) Experimental angular variations of H_{eb}^{FMR} (full squares) and of H_{eb}^{MAG} (empty circles).

The significant difference between the $H_{\text{res}}(\phi_H)$ curve for $t_{\text{Cu}} = 0.25$ nm and the others plotted in Fig. 2 indicates that when t_{Cu} increases, the coupling strength decreases and the $H_{\text{res}}(\phi_H)$ curves become typical of the case when $H_U < H_E \ll H_W$.¹³ The quite good coincidence between model and experiment confirms the above observations.

For $H_E \neq 0$, the EB field obtained from FMR measurements has been defined¹³ as $H_{eb}^{\text{FMR}}(\phi_H) = \frac{1}{2}[H_{\text{res}}(\phi_H) - H_{\text{res}}(\pi + \phi_H)]$ and, like H_{res} , strongly depends on the interaction strength. For high H_E/H_W ratios, its angular dependence becomes very close to that of H_{eb}^{MAG} ; they may, however, show rather different variations in the case of weak interactions (i.e., when $H_E \ll H_W$), depending on the H_U value as well.

H_{eb}^{FMR} versus ϕ_H , obtained using the measured $H_{\text{res}}(\phi_H)$ fields from Fig. 2, are plotted in Fig. 3 along with the experimental H_{eb}^{MAG} angular variations. Different from the data reported in the literature until now,^{4–11} these “field shifts,” obtained from different measurement techniques, coincide. The overlap between H_{eb}^{FMR} and H_{eb}^{MAG} is expected¹³ for H_E rather higher than H_U . Although such a coincidence is observed also for the other samples, one cannot conclude that they are strongly coupled from the analysis of their experimental curves only. The reason is that the error margin in the estimation, from the experiments, of both kinds of H_{eb} fields could be of the order of the difference between them when H_E and H_U are comparable in value.

The $H_{eb}(\phi_H)$ curves for the film with the thickest Cu spacer shown in Fig. 3 are exactly what one would expect for a very weakly coupled bilayer: while H_{eb}^{FMR} shows almost pure $\sin 2\phi_H$ variation, H_{eb}^{MAG} deviates from the sine behavior in the vicinities of $\phi_H = 0$ and π , as exemplified in Fig. 2(a) of Ref. 13.

Figure 4 shows the variations of J ($=tMH_E$), H_U , and H_{RA}^{FMR} vs t_{Cu} , obtained from the fittings. Both J^{FMR} and J^{MAG} decrease exponentially for $t_{\text{Cu}} \geq 0.25$ nm, i.e., $J \propto \exp(-t_{\text{Cu}}/\lambda)$, when t_{Cu} increases. The decay lengths λ are estimated to be $\lambda^{\text{FMR}} \approx 2.9$ Å and $\lambda^{\text{MAG}} \approx 3.1$ Å, values

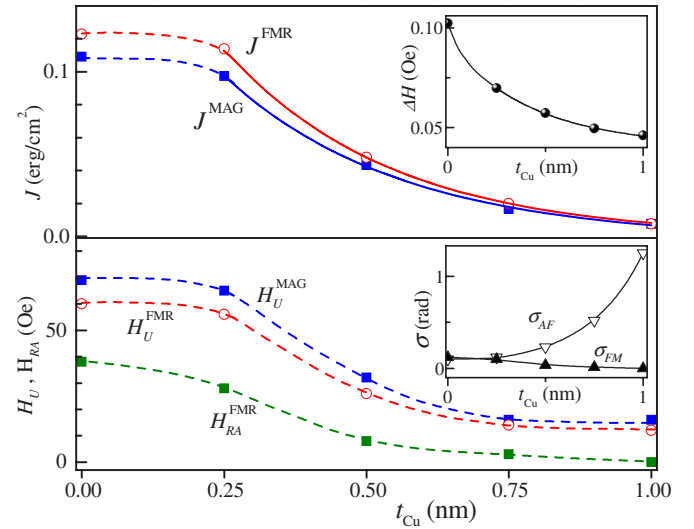


FIG. 4. (Color online) Spacer thickness dependencies of J , H_U , and H_{RA}^{FMR} as estimated by fitting the FMR and magnetization data. The FMR linewidth variation is plotted in the top-panel inset, and the bottom-panel inset shows the AF and FM easy axis distributions used in the magnetization curve fittings. The solid $J(t_{\text{Cu}})$ curves are best-fit results to exponential decay; all other curves are guides for the eyes.

rather smaller than those reported by Gökemeijer *et al.*² and comparable with those of Thomas *et al.*³ The short λ of a few angstroms indicates the so-called “short-range” coupling. The correct term, however, should be direct coupling, since it is, most probably, due to direct interfacial AF/FM contact through pinholes between the IrMn and Co layers, which normally occurs up to insertion layer thickness of ≈ 1 nm.^{3,20,21} As t_{Cu} gets thicker, the number of pinholes and their surface decrease and so does the effective coupling strength.

H_U and H_{RA} , however, after rapid initial decrease with t_{Cu} , remain almost constant for $t_{\text{Cu}} \geq 0.75$ nm. Remarkably, $J^{\text{FMR}} > J^{\text{MAG}}$ and $H_{RA}^{\text{FMR}} < H_{RA}^{\text{MAG}}$ for all t_{Cu} .

The thickness dependence of J and the anisotropy parameters of our samples are consistent with the following scenario. Let us start with the Co layer characteristics. Although both AF and FM layers are polycrystalline, the Co layer spin alignment is improved when increasing the thickness of the bottom-grown Cu layer due to the improvement of its crystallographic structure. This is corroborated by the gradual decreases with t_{Cu} of the FM easy axis distribution estimated from the magnetization curve simulations, σ_{FM} , shown in Fig. 4 and of the FMR linewidth, ΔH , also plotted in this figure. In polycrystalline materials, ΔH is increased because the dispersion in the anisotropy parameters (due to, e.g., interface roughness, defects, etc.) causes separate magnetic regions to resonate at different applied fields. Part of the ΔH decrease could also be attributed to the weakening of the coupling strength.²² Furthermore, ΔH could be interface dependent.²³

Contrary to the FM spin arrangement variation, the AF moment alignment becomes worse when t_{Cu} is increased, as indicated by the $\sigma_{\text{AF}}(t_{\text{Cu}})$ curve in Fig. 4. The increase of σ_{AF} with t_{Cu} at first sight may seem strange, since the IrMn layers

are deposited before the Cu ones. However, this increase is naturally explained, having in mind that the interfacial AF spins are not coupled directly to the field but to the FM magnetization. The AF/FM contact area decreases as the Cu layer gets thicker due to the decrease of the number and the surface of the pinholes, and so does the number of the AF spins possible to be aligned. Thus, the capability of magnetic annealing to form an AF collinear arrangement gradually decreases, despite the fact that IrMn is a cubic anisotropy material with four easy magnetization axes, i.e., with good potential for improving its spin alignment.

There are two coexisting fractions of grains at the AF part of the interface: magnetically stable and unstable AF grains.²⁴ In EB systems, the stability is predominantly determined by the coupling strength between these grains' moments and the adjacent FM domains. In FMR experiments, whether a magnetic moment is stable or not depends on its relaxation time τ relative to the period of the microwave excitation, τ_{res} . It has been shown¹⁹ that the exchange bias could be frequency dependent, i.e., $H_{\text{res}}(\phi_H)$ obtained at two different excitation frequencies on the same piece of sample could differ considerably, the curve being obtained at lower ω characteristic of strong exchange coupling and that measured at higher ω typical of weak interactions. The reason is that only grains with $\tau > \tau_{\text{res}}$ contribute to the exchange bias. Some of the moments which are stable in an FMR measurement are unstable in a magnetization curve trace, since the measurement time of the latter is longer than τ , thus explaining the effectively lower J^{MAG} value as compared to that extracted from the FMR technique.

AF grains with $\tau \approx \tau_{\text{res}}$ contribute to the rotatable anisotropy and not to the exchange bias in FMR measurement.^{6,24} Here, $H_{\text{RA}}^{\text{FMR}} = 2H_{\text{RA}}^{\text{MAG}}$ was used in the simulations for all samples, the cause being, once again, that responsible for $J^{\text{FMR}} > J^{\text{MAG}}$: due to their low τ values, some of the moments that contribute to $H_{\text{RA}}^{\text{FMR}}$ are "sensed" as superparamagnetic in a dc magnetization measurement.

Both FMR and magnetization techniques show that H_U rapidly increases with the decrease of t_{Cu} starting from $t_{\text{Cu}} \approx 0.75$ nm. It remains approximately constant for higher Cu thicknesses, where $J \approx 0$, which clearly indicates that the increase of H_U is an exchange-induced effect. This could be attributed to a presence of AF/FM subsystems with incompletely compensated AF interface along the effective easy axis of the sample, which results in an enhanced width of the hysteresis loops.²⁵ In the framework of our model, which does not account for configurations of the type where a FM moment is coupled to two AF sublattice moments, this enhancement is interpreted as an additional contribution to H_U . Since J becomes weaker with the increase of t_{Cu} , the role of this three-moment system decreases and, consequently, so does H_U .

The above considerations also explain the lower values of H_U estimated from FMR data as compared to those extracted from the magnetization curve fittings. Some of the AF grains with $\tau > \tau_{\text{res}}$, although stable for FMR and contributing to the EB, do not give an additional raise to H_U^{FMR} . They, however, contribute to H_U in the "slower" magnetization measurements.

In summary, we observed identical exchange-bias fields and different coupling strengths and anisotropy fields, obtained via FMR and magnetization measurements, when the direct coupling through pinholes in the Cu interlayer is not negligible in our IrMn/Cu/Co system. These features were attributed to magnetic layers with independent easy axis distributions, to the distinct measurement times of the techniques, and to the role of AF grains with different sizes and different magnetic stabilities at the AF side of the interface.

ACKNOWLEDGMENT

This work has been supported by the Brazilian agencies CNPq, FAPERGS, and CAPES.

¹W. H. Meiklejohn and C. P. Bean, *Phys. Rev.* **102**, 1413 (1956); **105**, 904 (1957).

²N. J. Gökemeijer, T. Ambrose, and C. L. Chien, *Phys. Rev. Lett.* **79**, 4270 (1997).

³L. Thomas, A. J. Kellock, and S. S. P. Parkin, *J. Appl. Phys.* **87**, 5061 (2000).

⁴B. H. Miller and E. Dan Dahlberg, *Appl. Phys. Lett.* **69**, 3932 (1996).

⁵V. Ström, B. J. Jönsson, and E. D. Dahlberg, *J. Appl. Phys.* **81**, 5003 (1997).

⁶R. D. McMichael, M. D. Stiles, P. J. Chen, and W. F. Egelhoff, Jr., *Phys. Rev. B* **58**, 8605 (1998).

⁷E. D. Dahlberg, B. Miller, B. Hill, B. J. Jönsson, V. Ström, K. V. Rao, J. Nogués, and Ivan K. Schuller, *J. Appl. Phys.* **83**, 6893 (1998).

⁸P. Miltényi, M. Gruyters, G. Güntherodt, J. Nogués, and Ivan K. Schuller, *Phys. Rev. B* **59**, 3333 (1999).

⁹H. Xi, R. M. White, and S. M. Rezende, *Phys. Rev. B* **60**, 14837 (1999).

¹⁰J. R. Fermin, M. A. Lucena, A. Azevedo, F. M. de Aguiar, and S. M. Rezende, *J. Appl. Phys.* **87**, 6421 (2000).

¹¹R. L. Rodríguez-Suárez, L. H. Vilela Leão, F. M. de Aguiar, S. M. Rezende, and A. Azevedo, *J. Appl. Phys.* **94**, 4544 (2003).

¹²J. Geshev, *Phys. Rev. B* **62**, 5627 (2000).

¹³J. Geshev, L. G. Pereira, and J. E. Schmidt, *Phys. Rev. B* **64**, 184411 (2001).

¹⁴S. Nicolodi, L. C. C. M. Nagamine, A. D. C. Viegas, J. E. Schmidt, L. G. Pereira, C. Deranlot, F. Petroff, and J. Geshev, *J. Magn. Magn. Mater.* (to be published).

¹⁵S. Nicolodi, L. G. Pereira, J. E. Schmidt, L. C. C. M. Nagamine, A. D. C. Viegas, C. Deranlot, F. Petroff, and J. Geshev, *Physica B* **384**, 141 (2006).

¹⁶D. Mauri, H. C. Siegmann, P. S. Bagus, and E. Kay, *J. Appl. Phys.* **62**, 3047 (1987).

¹⁷J. Geshev, L. G. Pereira, and J. E. Schmidt, *Phys. Rev. B* **66**, 134432 (2002).

¹⁸J. Camarero, J. Sort, A. Hoffmann, J. M. García-Martín, B. Dieny, R. Miranda, and J. Nogués, *Phys. Rev. Lett.* **95**, 057204

- (2005).
- ¹⁹J. Geshev, L. G. Pereira, J. E. Schmidt, L. C. C. M. Nagamine, E. B. Saitovitch, and F. Pelegrini, *Phys. Rev. B* **67**, 132401 (2003).
- ²⁰Y. G. Yoo, S. G. Min, and S. C. Yu, *J. Magn. Magn. Mater.* **304**, e718 (2006).
- ²¹J. Wang, *J. Appl. Phys.* **91**, 7236 (2002).
- ²²R. D. McMichael, M. D. Stiles, P. J. Chen, and W. F. Egelhoff, Jr., *J. Appl. Phys.* **83**, 7037 (1998).
- ²³S. Mizukami, Y. Ando, and T. Miyazaki, *Phys. Rev. B* **66**, 104413 (2002).
- ²⁴E. Fulcomer and S. H. Charap, *J. Appl. Phys.* **43**, 4190 (1972); M. D. Stiles and R. D. McMichael, *Phys. Rev. B* **59**, 3722 (1999); **63**, 064405 (2001).
- ²⁵R. E. Camley, B. V. McGrath, R. J. Astalos, R. L. Stamps, Joo-Von Kim, and Leonard Wee, *J. Vac. Sci. Technol. A* **17**, 1335 (1999).